

## 2-9 Prediction Method and Proof Measurement of LF Standard Frequency Waves

TSUCHIYA Shigeru, IMAMURA Kuniyasu, ITO Hiroyuki, MAENO Hideo,  
KUBOTA Minoru, and NOZAKI Kenro

Numerical method to predict low frequency field strength was developed based on the worldwide measurement of LF standard frequency waves, and was accepted to revise the corresponding description in the recommendation of the International Telecommunication Union Radiocommunication Sector (ITU-R). Revised recommendation is suitable to predict the LF field strength up to 16,000 km by means of wave hop method. The measured range variation, diurnal variation, and interference between ground wave and sky waves are fairly agreed with the prediction. The wave hop method is shown to be applicable down to 40 kHz, whereas waveguide method is recommended below 60 kHz in the recommendation. A new sensitive and highly discriminative receiving system is under development for the long distance propagation including higher-order ionospheric reflection modes and many kinds of noise.

### **Keywords**

LF, Standard frequency wave, Field strength, ITU-R field strength prediction method, Wave hop method

### **1 Introduction**

National Institute of Information and Communications Technology (NICT) transmits 40 kHz and 60 kHz LF standard frequency waves (JJY) from Ohtakadoya-yama in Fukushima Prefecture and Hagane-yama on the Saga-Fukuoka Prefecture boarder respectively<sup>[1][2]</sup>. Due to their advantage of long range propagation, easiness to penetrate building walls and stability, LF band waves have been increasingly used for operations related to standard frequency and time signals (SFTS) in recent years and there has been a tendency to promote construction of new transmitting stations around the world. Consequently, there has been the threat of interference by sharing or neighboring frequencies. It is reported that overseas travelers have experienced their clocks switching between Japan time and US time depending on

the time of a day. There are reports on JJY reception from as far away as the U.S. West Coast, Europe and New Zealand.

In general, the synthetic waves of ground waves propagating along the ground and sky waves reflected at the bottom of the ionospheric region are received in the LF band. Although ionospheric variation due to solar and geomagnetic activity less affects LF propagation in comparison to MF and HF band radio waves, severe solar and geomagnetic activities<sup>[3]</sup> and fluctuations in the lower atmosphere<sup>[4]</sup> sometimes disturb LF propagation. Electric field strength of LF radio wave under quiet conditions is calculated according to International Telecommunication Union Radiocommunication Sector (ITU-R) Recommendation P. 684-5 “Prediction of field strength at frequency below 150 kHz”<sup>[5]</sup>. However, the waveguide mode method for calculations is recommended for

frequencies less than 60 kHz and the wave hop method is recommended for frequencies of 60 kHz or more in the Recommendation.

In 2004, NICT surveyed the field strength all around Japan from Hokkaido to Okinawa in order to investigate the propagation condition and the reception quality of JJY40 and 60 kHz<sup>[6][7]</sup>. For analysis of the measured data, the short-range LF field strength prediction method developed to cover the transmission range of two hops or within approximately 4,000 km was used, which showed a good correspondence to the measured data in terms of the range and the diurnal variations. It was also shown that the measured MID (Maximum Interference Dip)<sup>[8]</sup>, which was caused by the interference of ground and sky waves, was consistent with the prediction when the reflection altitude was 69.4 km.

In the short-range LF field strength prediction method, we adopted the parabolic layer model for the ionospheric D region that reflects sky waves and the path length of the sky waves was calculated based on the model. Furthermore, the absorption is controlled by the solar zenith angle in the revised ITU-R Recommendation, then the field strength is predicted at any time of a day in any season of a year<sup>[9][10]</sup>. Previous predictions of sky wave field strength less than 150 kHz requiring much time and effort using charts and tables were only capable under restricted conditions such as night-time and daytime in summer and winter. As a result of this Recommendation revision, predictions have become possible at any time of the day by setting the parameters on a PC.

As the next step, an algorithm capable of calculating up to 10 hops and 16,000 km was developed and verification measurement was performed using an on-board receiving system focusing on LF long range propagation property between Japan and the United States and Japan and Antarctica from 2007 until 2009<sup>[11][12]</sup>. These results were then used to perform next revision of the ITU-R recommendation<sup>[5][13]</sup>. The PC based numerical calculation method up to 2 hops and 10 hops in order is compiled after the section of former calculation method using

charts and tables in the wave hop method chapter of the latest recommendation.

The on-board observations succeeded in measuring the transition of the JJY 60 kHz standard radio wave to the WWVB 60 kHz United States standard radio wave as the ship approaching to the United States<sup>[11][12]</sup>. However, as it turned out that atmospheric noise and city noise dominated over long distances, an alternative receiving system with a lock-in amplifier for highly sensitive and highly selective signal detection is under development substituting for the conventional measurement system with a commercial receiver.

In this paper, we will first provide an outline of the LF field strength prediction method adopted in the ITU-R recommendation. Then, we will discuss the measurement system and show the short range results measured around Japan and the long range results measured by the on-board system. Finally, we will show the lock-in amplifier type highly sensitive receiving system currently being developed by learning from the previous experiences, and discuss the trend of improving the prediction method.

## 2 The LF field strength calculation method

The current ITU-R recommendation<sup>[5]</sup> includes both the wave hop method and the waveguide mode method and it recommends the waveguide mode method for the frequency lower than 60 kHz and the wave hop method for higher frequency. In the waveguide mode method possible modes of radio wave propagate between the earth and the ionosphere analogous to a waveguide of microwave without a wall. Although it is suitable to predict for a low frequency standing less than several wavelengths between the earth and the ionosphere, it cannot calculate in vicinity of the transmitting point. In the wave hop method the field strength of the received signal is the synthesis of many rays reflected between the ground and the ionosphere. The wave hop method is intuitively understandable but the radio wave spread into the space is not considered. The field strength pre-

diction method that we developed synthesizes ground waves and sky waves up to ten reflections using the wave hop method.

When the radio waves, transmitted with vertical polarization, propagate preserving polarization at each reflection point, effective field strength  $E$  (mV/m) at the loop antenna on the ground can be expressed by the synthesized field strength of sky waves up to ten reflections ( $Es_K$ ) and ground waves ( $Eg$ ) as follows:

$$E = Eg + \sum_{K=1}^{10} Es_K \quad (1)$$

The received field strength is calculated by vector sum as the sky waves and ground waves include phase terms due to propagation distance.  $Eg$  corresponding to subjective propagation distance is calculated through the interpolation taken from the numerous charts provided in ITU-R Rec. P.368-7[14]. Relative permittivity  $\epsilon$  and electric conductivity  $\sigma$  are selected from sea water ( $\epsilon: 70, \sigma: 5$  S/m), land ( $\epsilon: 22, \sigma: 0.003$  S/m) and dry earth ( $\epsilon: 7, \sigma: 0.0003$  S/m) as the earth condition, and frequency is interpolated from 40, 50, 75, 100, 150, 200, 300, 400 and, 500 kHz. Sky wave field strength  $Es_K$  for the  $K$ -times reflections is denoted by:

$$Es_K = \frac{600\sqrt{Pt} \cos(\Psi_K) \prod_{L=1}^K Rc_{K,L}}{\sum_{L=1}^K Pl_{K,L}} Fc_K Rg_K^{K-1} Ft_K Fr_K \exp\left(-jk \sum_{L=1}^K Pl_{K,L}\right) \quad (2)$$

where  $j$  is the imaginary unit and  $k$  is the wave number of radio waves, and the suffix  $K$  and  $L$  refer to number of hops and number of reflection points each. The reflection points are simply set at equally divided distances of the ground without considering gradient of the ground or the slanted ionosphere.  $Pt$  (kW) is the effective radiation power and  $\Psi_K$  denotes the elevation angle of  $K$  hop waves. The earth reflection coefficient  $Rg_K$  is calculated for the vertical polarized effective reflection coefficient of conductive ground[15]. Here, relative permittivity and electric conductivity of the ground are provided as parameters. The solar zenith angle  $x$  and the ionospheric incident angle  $i$  are calculated at each ionospheric reflection

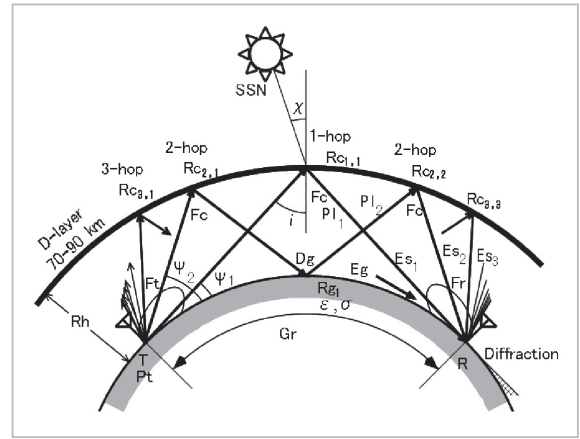


**Fig.1** Schematic diagram of wave hop method

tion point and then the ionospheric reflection coefficients  $Rc_{K,L}$  are derived. The propagation path length of each hop  $\sum_{L=1}^K Pl$  is calculated when the ground distance and reflection altitude  $R_h$  is determined.  $R_h$  is determined by the electron density distribution at the bottom of the ionospheric region. Parabolic distribution model of D-layer we introduced for calculating the reflection altitude will be explained in 2.1. Figure 1 shows a schematic diagram of the propagation and the parameters will be discussed below.

## 2.1 Reflection altitude model

Assuming a parabolic electron density distribution in the ionospheric D/E region, the maximum plasma frequency is calculated using the ITU-R Rec. P. 1239[16]. Then, on the condition that the lowest plasma frequency  $f_b$  is 10 kHz, when the minimum semi-layer thickness  $y_{min}$ , maximum semi-layer thickness  $y_{max}$  and the maximum altitude  $h_{max}$  for the E layer is 10 km, 30 km, and 100 km respectively, the minimum reflection altitude at night is 90 km ( $h_{max} - y_{min}$ ) and 70 km ( $h_{max} - y_{max}$ ) during the day.

For example, h-f (frequency to reflection altitude) profiles at a certain point are shown in Fig. 2. In the figure, identical profiles are assumed between 12:00 am and 3:00 am LT.

The reflection altitude  $R_h$  is calculated as follows.

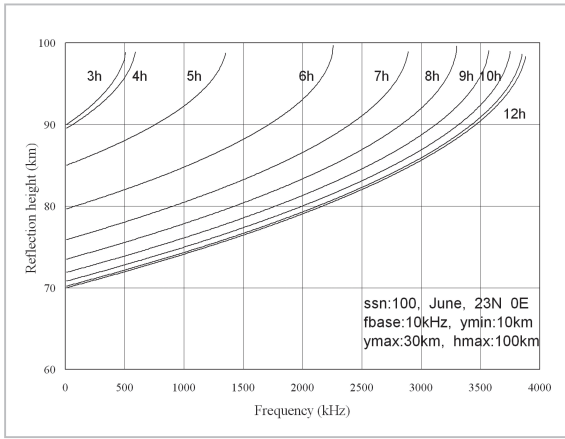


**Fig.2** Ionospheric reflection altitude model

$$R_h = h_{\max} - ym \sqrt{1 - \frac{f - f_b}{foE}} \quad (3)$$

where

$$ym = ymm - \frac{(ymm - y_{\min})(f_{\max} - foE)}{f_{\max} - f_{\min}} \quad (4)$$

and  $ymm$  is calculated from

$$ymm = y_{\max} - \frac{(y_{\max} - y_{\min})(fk0 - f_{\max})}{(fk0 - f_{\min})} \quad (5)$$

Where,  $fk0$  ( $foE$  at the solar zenith angle 0),  $f_{\max}$  (the maximum value of  $foE$  at that point) and  $foE$  (at the local time) can be calculated from the Chapter 4:  $foE$  prediction in the reference [16].

## 2.2 Focusing factor $Fc_k$

With the spherical earth and spherical ionosphere models, the focusing effect occurs at the ionospheric reflection and defocusing effect at the ground reflection. Assuming that they cancel out each other for convenience, focusing factor  $Fc_k$  at ionospheric reflection is counted once. Although there were individual curves for daytime and nighttime in the previous ITU-R recommendation, averaged curves now enable to be calculated 24 hours per day. Averaged focusing factor is shown in Fig. 3 providing frequencies as parameters.

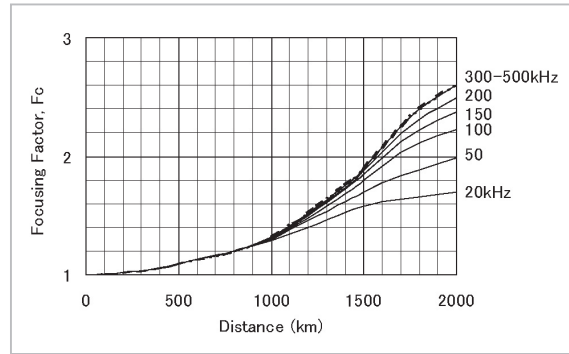


**Fig.3** Focusing factor (based on the reference [5])

**Table 1** Geodetic constants

Ground condition	Relative permittivity, $\epsilon$	Conductivity, $\sigma$ (S/m)
Sea	80	5
Land	15	0.002
Dry ground	15	0.0005

## 2.3 Antenna factors $Ft_k, Fr_k$

Transmitting antenna factor  $Ft_k$  and receiving antenna factor  $Fr_k$  are evaluated by interpolation for elevation angles and frequencies from the antenna factor curves provided in the reference[5] on three ground conditions in Table 1. Negative elevation angles bring about diffracted waves and, diffraction losses are included in these antenna factor curves.

## 2.4 Ionospheric reflection coefficient $Rc_{k,L}$

The ionospheric reflection coefficients  $Rc_{k,L}$  at each reflection point are expressed as a function of  $f \cos(i)$  for minimum (SSN: 0 – 25), medium (SSN: 25 – 75) and maximum (SSN: 75 – 150) solar activities shown in Fig. 4(a) to (c). The arbitrary propagation conditions are evaluated by the interpolation from these three figures. Here,  $f$  is the frequency and  $i$  is the incidence angle into the ionosphere.

## 3 LF SFTS field strength measurement

The standard radio wave field strength at 40 kHz and 60 kHz was measured across the country and compared with the predicted values us-

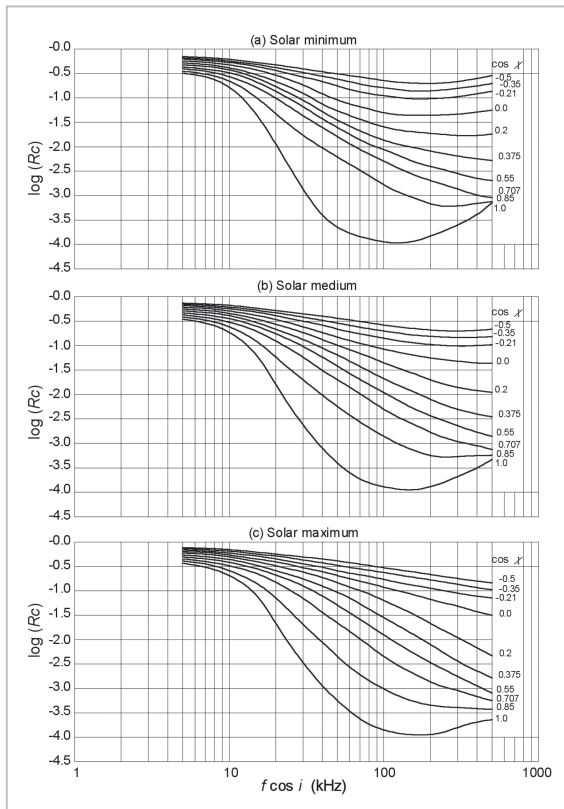


**Fig.4** Ionospheric reflection coefficients

Ionospheric reflection coefficients of (a) the minimum (SSN: 0 – 25), (b) the medium (SSN: 25 – 75), and (c) the maximum solar activity period (SSN: 75 – 150) taking the solar zenith angle as parameters.  $f$  (kHz) and  $i$  of the horizontal axis denotes frequencies and ionospheric incidence angles respectively. Ionospheric reflection coefficients for  $\cos(x) = -0.5, -0.35, -0.21, 0.0, 0.2, 0.375, 0.55, 0.707, 0.85, 1.0$  are plotted from top to bottom (based on the reference [5]).

ing the numerical field strength prediction method. 60 kHz SFTS is also transmitted in the United States. The main specifications for the SFTS stations are shown in Table 2.

Up to several hundred kms, ground wave is superior in LF propagation, but ionosphere reflected sky waves gradually prevail as the propagation range increases. In Japan, two times reflections are sufficient to be considered and the two times reflection model was used for domestic measurements discussed below.

### 3.1 Domestic ground based field strength measurement

Ground based measurement was conducted from January to February 2004. Using a loop antenna and a field strength meter, fixed-point measurements were performed to measure diurnal variation at selected points every 100 km from the transmitting stations and mobile measurements were performed to measure range variation using moving vehicles. The measurement points are shown in Fig. 5.

The detailed results of the measurement are in the references [6][7][9][12]. Measured range variation, diurnal variation, and MID[8] in the field strength well agreed with the predicted values incorporating up to two reflections. Examples of the predicted and measured range variations of the field strength are shown in Fig. 6.

The 40 kHz and 60 kHz JJY effective radiating powers are decided from the field strength measured at the 100 km and 200 km from the transmission station and were 12.5 kW and 25

**Table 2** Specifications for transmitting stations of LF standard radio waves

Station	JJY	JJY	WWVB
Location	Ootakadoya-yama Fukushima Pref. JAPAN	Hagane-yama Saga/Fukuoka Pref. JAPAN	Fort Collins Colorado, U.S.A.
Latitude	37°22'21"N	33°27'56"N	40°40'N
Longitude	140°50'56"E	130°10'32"E	105°03'W
Antenna facility	Umbrella top loading antenna	Umbrella top loading antenna	Top-loaded monopole
Antenna height	250 m	200 m	122 m(2×4)
Eff. Rad. P.	12.5 kW	25 kW	70 kW
Carrier frequency	40 kHz	60 kHz	60 kHz
Modulation	A1B	A1B	A1B
Frequency accuracy	$\pm 1 \times 10^{-12}$	$\pm 1 \times 10^{-12}$	$\pm 1 \times 10^{-12}$

kW respectively. In this paper, these values are used for JJY transmitted power.

Although the wave hop method is recommended to be applied for frequency higher than 60 kHz in the ITU-R Rec. P. 684, our measurement proved that it was applicable for 40 kHz with a sufficient accuracy. In addition, it turned

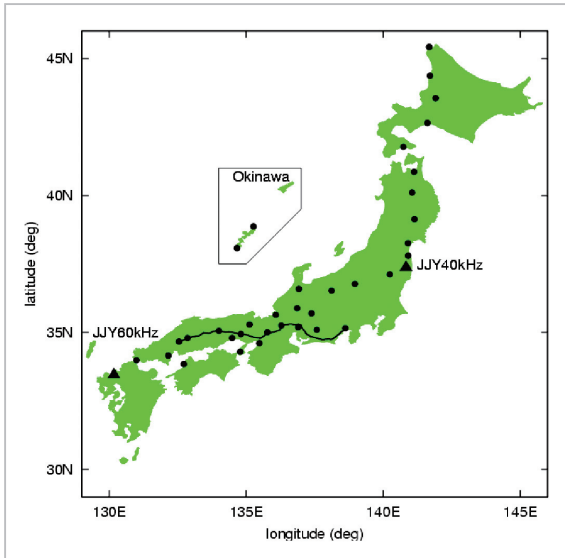


**Fig.5** Domestic field strength measurement points

Fixed measurement points (●), moving measurement course (bold line), and JJY stations (▲)

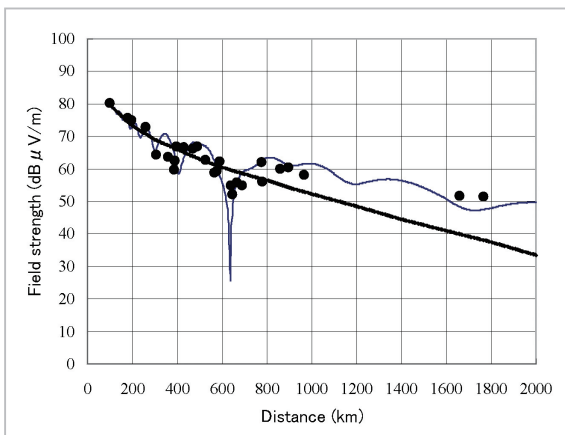


**Fig.6** Range variation of JJY 40 kHz field strength in daytime

(●) denote measured values, and the bold and thin lines denote the predicted values of ground waves and of the synthesized field strength up to 2 reflections respectively (based on the reference [12])

out that the measured field strength exceeded 50 dB $\mu$ V/m throughout the country to assure that commercial radio controlled clocks and watches automatically set the time.

### 3.2 Mobile measurements by means of ships

#### 3.2.1 Measurement system

A system for automatically measuring field strength and phase for 24 hours per day was developed and installed on oceangoing ships[11]. Since the bearing to the transmitting station changes as the ship cruises, the on-board antenna should be azimuthally omnidirectional. We developed a tri-axis crossed loop antenna and attached it to a handrail near the laboratory on the ship. Azimuthal deviation of the receiving loop antenna was within  $\pm 0.3$  dB in all directions. A block diagram of the measurement system is shown in Fig. 7.

The field strength meter samples one hundred data every 0.1 seconds for antenna X, Y, and Z axes in order at each 40 kHz and 60 kHz, and conducts calibration for each frequency using a reference oscillator. It takes about three minutes to repeat the sequence above. The bandwidth of the field strength meter was 200 Hz and its sensitivity was approximately 30 dB $\mu$ V/m. The square root of the square sum of the upper decile value of one hundred data for each axis was recorded as quasi peak (QP) field strength.

This system was installed on the Antarctic

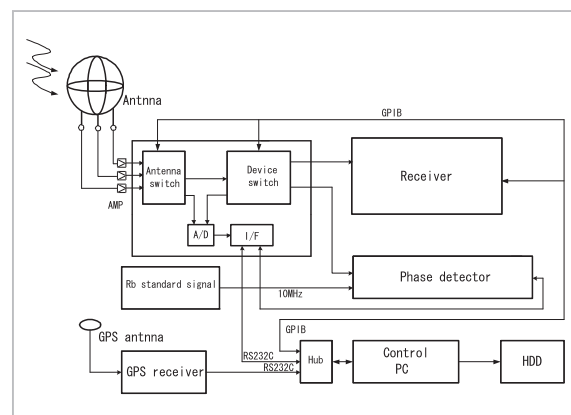


**Fig.7** Block diagram of the on-board measurement system with field strength meter

research expedition icebreaker “Shirase” and measurements were conducted in 2006 and 2007 training cruises around Japan and during the round-trip for the 49<sup>th</sup> Japanese Antarctic Research Expedition starting in 2007. The system was installed on container ship “Argus” of Nippon Yusen Co., Ltd. and measurements were conducted in South East Asia and North America cruise in 2007. The onboard measurement cruise courses are shown in Fig. 8.

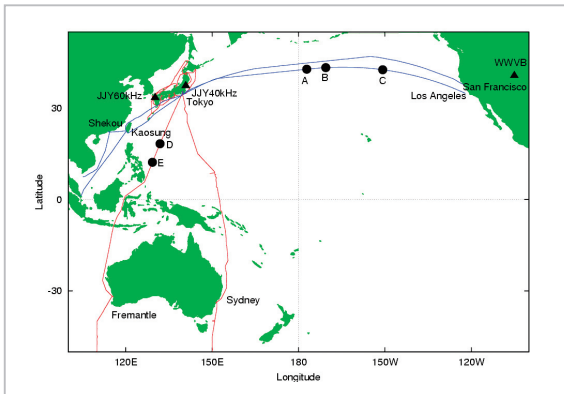


**Fig.8** Routes of on-board mobile measurement

Red line: training cruise courses (2006, 2007) and Antarctica course by the “Shirase” (2007)  
 Blue line: South-East Asia and Trans Pacific Ocean courses by the “Argus” (2007)

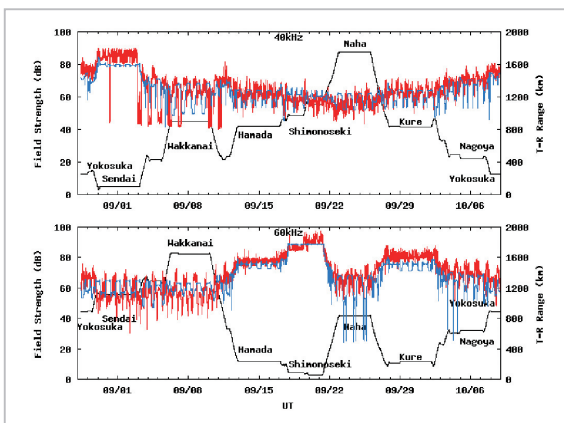


**Fig.9** Variation of field strength during the training cruise of the “Shirase” (2007)

Upper case: 40 kHz  
 Lower case: 60 kHz  
 The red denotes quasi-peak (QP) values every 3 minutes, the blue line is the predicted field strength, and the black is the great-circle distance from the transmitting station.

### 3.2.2 Measurements around the coast of Japan

Ground wave and synthesized sky waves up to two reflections above Japan are the main components of field strength. As there is no fading caused by ionospheric fluctuations in sky waves there are no differences between the QP and MD (Median) in measured field strength except sunrise and sunset. Figure 9 shows the records of the training cruise around the coast of Japan on the “Shirase” in 2007. The red line represents the QP, the blue line represents the prediction calculated up to two reflections and the black line represents the great-circle distance from the transmitting station. From September 3 to 7 and September 10 and 11 JJY 40 kHz was suspended for maintenance in the daytime. The measured field strength of 40 kHz anchoring at Sendai and 60 kHz at Kure were higher than expected by several dB, which was supposedly due to man-made noise near urban areas. The measurement and predicted field strength agree during the cruise (the declining portion of the black line) and other ports.

### 3.2.3 Long distance mobile measurements

After a round trip to Singapore leaving Tokyo Oi Wharf on May 13, 2007, the “Argus” equipped with a measurement device made another round trip from far out over Japan to the U.S. West Coast and arrived back in Oi Wharf on June 24. Figure 10 shows the field strength during the trans-Pacific cruise to and from Japan along the greatcircle. The red line shows the measured field strength, the blue line represents the prediction using the numerical field strength prediction method and the green line represents the atmospheric noise level of every four hours. In addition, the black line shows the great-circle distance from the JJY station.

On the assumption that long distance propagated radio signal fluctuates according to the Rayleigh distribution, received signal level was converted to MD after subtracting 5.2 dB from the QP then a moving average of fifteen samples (approximately 45 minutes) is presented as measurement. ITU-R Rec. P. 372<sup>[17]</sup> includes twenty four global maps on atmospheric

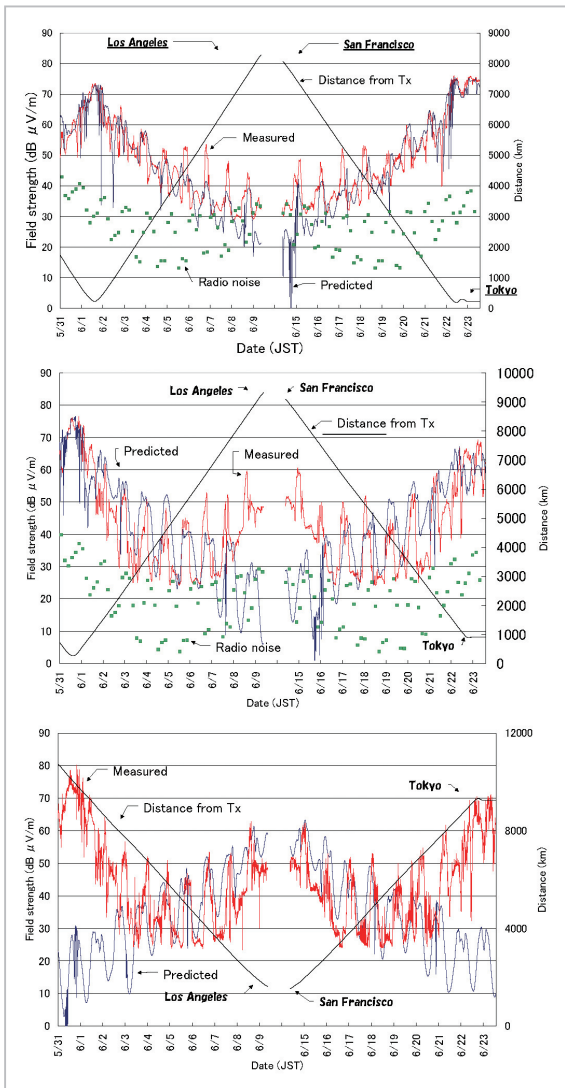


**Fig.10** Field strength on the Pacific route (Upper: 40 kHz, Middle: 60 kHz-JJY, Lower: 60 kHz-WWVB)

Red line: measured field strength  
 Blue line: calculated field strength  
 Green dots: atmospheric noise level (based on the reference [17])  
 (Cited from reference [12])

noise figure distribution below HF band for each season and local times. After reading out the noise factor  $F_{am}$  of the location of measurement, the following equation determines noise level by compensating the receiver bandwidth and the frequency.

$$En = F_{am} - 155.5 + 20 \log f + 10 \log b \quad (6)$$

where  $En$  (dB $\mu$ V/m) is median of the noise lev-

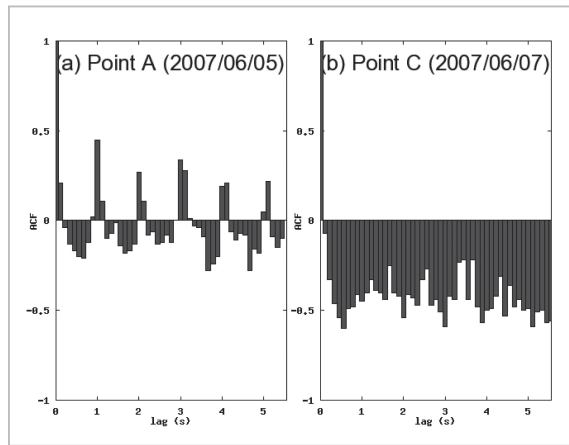


**Fig.11** Autocorrelation coefficients of the 40 kHz reception signal strength

(a) Point A on the route (June 5)  
 (b) Point C on the route (June 7)  
 (Cited from reference [12])

el in bandwidth  $b$  (Hz) and  $F_{am}$  is the noise figure for 4-hour-time block at the center frequency  $f$  (kHz). Since the measurement on the Pacific route was conducted from spring to summer, the  $F_{am}$  was averaged for spring and summer every four hours and  $En$  was determined for the system bandwidth  $b = 200$  (Hz).

The signal strength of LF standard waves is approximately the same level as a background noise beyond 4,000 km. Although the existence of signals can be confirmed by hearing the call sign every hour, great effort and listening technique are required. Signal determination by autocorrelation coefficient method was introduced utilizing SFTS modulation in amplitude every second with long or short pulse width. The autocorrelation coefficients for a series of one hundred pulse trains which were being sampled approximately every 0.1 second were evaluated; they were determined as standard waves when one second periodicity was detected and otherwise decided as interference or noise.

Although the 40 kHz measurement agreed with the prediction up to approximately 4,000 km from the transmitting station on the Pacific route from Japan to the U.S. West Coast, it came close to the atmospheric noise level which is the sensitivity limit beyond the said distance. The signal strength on June 5, 2007

indicated at Point A in Fig. 8 was sufficiently higher than the noise level, thus well matched the predicted value and the autocorrelation shows the periodicity of one second (Fig. 11 (a)). Conversely, the signal strength on June 7, two days later, indicated at Point C in Fig. 8 was affected by the background atmospheric noise and the autocorrelation in Fig. 11 (b) shows a negative value without periodicity.

While the field strength of 40 kHz declined with the distance, the 60 kHz wave field strength became increased again from the south of the Aleutian Islands. It should be attributed to the US standard wave WWVB transmitted with 60 kHz same as JJY. The 60 kHz measurement and prediction of WWVB waves for the entire course are shown in the lower case of in Fig. 10. The autocorrelation coefficients on June 5, when the JJY 60 kHz and the WWVB 60 kHz level approached almost the same level (point A in Fig. 8), showed uniform positive values without periodicity. Twelve hours later at point B in Fig. 8, the WWVB began to increase and the periodicity reemerged one second in the autocorrelation coefficients. From the above, it is clear that waves which became stronger as getting closer to the U.S. West Coast were the WWVB.

As shown in the center and bottom cases in Fig. 10, the measured and predicted field strength for 60 kHz wave over the Pacific Ocean route matched extremely well.

The Antarctic expedition ship “Shirase” left Tokyo on November 14, 2007 and arrived in Fremantle, on the west coast of Australia, on November 28. She then left the port on December 3, headed first south and then along the Antarctic coast for the Syowa Station. On the return route, the “Shirase” departed the Syowa Station on February 15, 2008 and arrived in Tokyo on April 12 after stopping at Sydney from March 20 to March 26. The transmission distance exceeds 9,000 km and signal strength became weak beyond Australia. However, JJY waves were detected and confirmed for a few days. Figure 12 shows the received and predicted field strength, atmospheric noise level, and the great circle distance from the transmit-

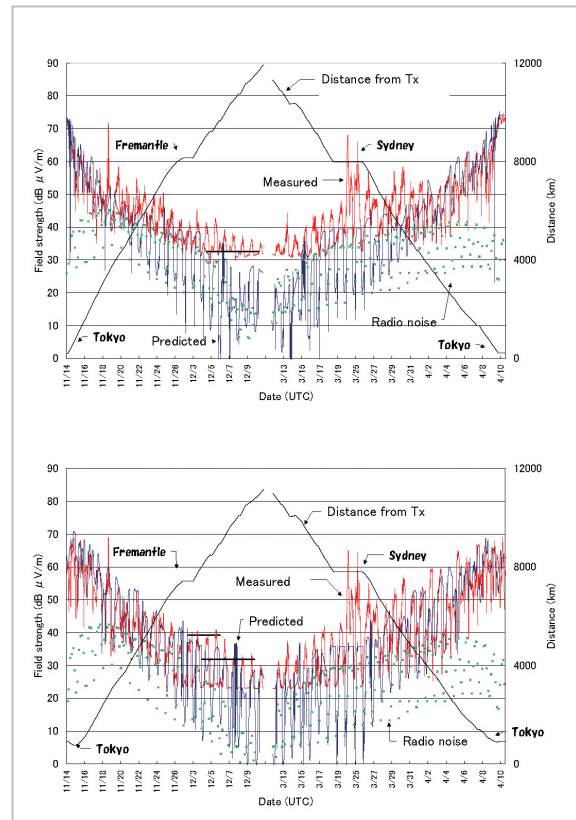


**Fig.12** Comparison between the measurement and predicted values of field strength on the Antarctic route

Upper: 40 kHz  
 Lower: 60 kHz  
 (Cited from reference [12])

ting station on the Antarctic route for 40 kHz (top) and 60 kHz (bottom). The left half of each chart shows the outward route from Japan via Fremantle and the right half shows the return route to Japan via Sydney. Although the Antarctic route did not run along with the great circle as the Pacific Ocean route, the passage of time was approximately proportional to the propagation distance.

The received signal level of 40 kHz increased from around November 18, 2007 passing east of the Philippines to south and it remained at a high level until Fremantle with the fast noisy fluctuations. According to the autocorrelation coefficient method, the periodicity of autocorrelation coefficients that resulted from time code of one second was clearly apparent in the JJY 40 kHz reception strength autocorrelation coefficient on November 17

(course point D). Conversely, negative correlation coefficient appeared with no periodicity on November 18 (course point E) due to noise. Furthermore, atmospheric noise predicted in the reference [17] increased close to signal level. Therefore, it is apparent that most of the reception data until Fremantle from November 18 was contaminated by atmospheric noise. However, signal periodicity was confirmed for both 40 kHz and 60 kHz only on November 24. Furthermore, after leaving Fremantle, the 60 kHz signal was last confirmed on December 6 at the distance of about 9,300 km from the transmitting station.

During the returning cruise, 60 kHz signal was recognized only from March 15 to March 17 on the way from Antarctica to Sydney. The furthest distance point was 50 degrees south, 9,600 km from transmitting station. Since then, signals could not be recognized due to the contamination of city noise around Sydney and atmospheric noise around Papua New Guinea. JJY waves were received from April 2 after crossing the Equator.

As SFTS radio signals were interfered by tropical atmospheric noise throughout the entire Antarctic route, constant measurement for 40 kHz waves could be obtained particularly only up to approximately 2,000 km on the outbound route and approximately 4,000 km on the return route. However, 60 kHz signal was able to receive for approximately 8,000 km on both back and forth routes with the equivalent level of prediction. Also, strong man-made noise disturbed both 40 kHz and 60 kHz receiving while passing near large cities.

#### 4 The development of highly sensitive receiving system

The above receiving system was designed based on field strength measurements for domestic in Japan. As a result, it is not sensitive enough to perform observations over long distances. In addition, separation of signals from fading, noise and interference, all of which are not a problem with manual observations in Japan, are essential requirements for automatic

measurement. Signals were determined by the presence of one-second periodicity in the auto-correlation coefficients on the Pacific and Antarctic cruise. However, phase tracking, Amplitude Probability Distribution (APD) plot, and neighboring spectrum analysis are preferable in order to determine signal levels among interferences. Using APD and spectrum analysis to discriminate SFTS from standard radio waves and noise/interference, Iwama et al. showed that noise/interference were sometimes stronger than standard radio waves in Tokyo [18].

Figure 13 shows the measurement for the “Argus” South East Asia outbound route from Tokyo to the coast of Thailand via Kao-Hsiung (Taiwan) and Shekou (Hong Kong) in 2007. The quasi-peak (QP) values and median (MD) values were determined using one hour data. Difference between QP and MD appeared beyond about 3,000 km showing that fading was coming up. In addition, increases in the reception level at each port suggest strong city noise. Receiver sensitivity of around 30 dB $\mu$ V/m is insufficient to discriminate the SFTS for analysis at noise increased low latitude.

The receiver sensitivity depends on its bandwidth and it is technically difficult to make the IF bandwidth considerably narrow. In order to clear the problem, a lock-in amplifier was

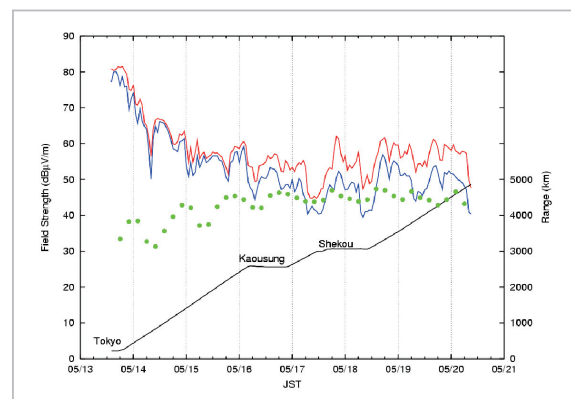


**Fig.13** Measurement values of 40 kHz for the outbound route to South-East Asia

Red line: Quasi-peak (QP) values for 1 hour  
 Blue line: Median (MD) values for 1 hour  
 Green line: Atmospheric noise levels  
 Black line: Great-circle distance from the transmitting station



pect that the lock-in amplifier receiving system currently being developed will continuously receive signals beyond 10,000 km. Furthermore, we also expect highly accurate analysis by signal discrimination using phase tracking and APD analysis.

Since long range propagation of LF radio waves depends on many factors such as solar activity, seasons, time of a day, and transmitting conditions, it is necessary to continue experiments under various transmitting and ground conditions and to improve propagation theory. The measurements acquired so far are only worthy to verify one of the three solar activities shown in Fig. 4. Therefore, it is necessary to accumulate data for at least one solar cycle.

Although the prediction method in the ITU-R recommendation has been greatly improved since the manual calculation age, repeated revisions have caused the mixture of manual method, 2 hop numerical and 10 hop numerical. It is therefore necessary to arrange and rewrite the content. Since the existing calculation method was dragged on when the numerical method was introduced, the different values on ground conductivity were used for calculating ground waves, for antenna coefficients, and for ground reflection factors of sky waves. A map of the relative ground conductivity is adopted in the ITU-R Rec. P. 832[19]. It will be convenient to adopt these results for future recommendation to be consistent. If the map data is incorporated into an algorithm, relative permittivity and conductivity of each ground reflecting point can be automatically input, while the representative values on the propagation path is input manually in the current specifications. Since PCs of the day have increased processing capacity and data recording volumes, there are no obstacles to include map data into files. The ground wave calculation software is published by the ITU-R and it is preferable to be adopted in our prediction method.

The sunspot number (SSN) is customarily used for the parameter that affects the ionospheric activities. Ionization at the bottomside of the ionosphere is controlled by the soft X-ray to ultra-violet radiation. The radiation of this wavelength is suitably represented by 2,800 MHz solar radio emission (F10.7) rather than by SSN. The F10.7 is observed every day at Penticton Observatory in Canada and published by NOAA. In addition, the F10.7 is also observed by NICT and these parameters can be automatically acquired through the network as a continual solar activity index while a three-level SSN activity chart is utilized in current prediction method. Furthermore, modeling of the bottomside of the ionospheric region is also studied, therefore, it will be necessary to incorporate the results into the calculation algorithms step by step together with verifications using worldwide measurements. The development of the high sensitive receiver is just one step.

## Acknowledgements

The implementation of PC based LF field strength prediction method and the incorporation of multi reflection waves into the prediction algorithm were performed under the leadership of the late Dr. N. Wakai, former director general of the Radio Research Laboratory. The authors are instructed in both propagation theory and radio measurements by him. We would like to express our deep gratitude to Nippon Yusen Co., Ltd. who provides the container ship "Argus" for measurements on the South East Asia and Pacific Ocean routes over one month. We would also like to sincerely thank Kyoritsu Corporation for their cooperation on transporting and installing measurement system. The measurements on the Antarctic route were conducted by the 49<sup>th</sup> and 50<sup>th</sup> Japanese Antarctic Research Expedition Projects.

## References

- 1 N. Kurihara, "5-3 JJY, The national standard on time and frequency in Japan," *Jour. NICT*, Vol. 50, Nos. 1/2, pp. 179–186, 2003.
- 2 K. Imamura, N. Kotake, S. Tsuchiya, and K. Nozaki, "LF standard time and frequency transmission facilities and LF field strengths," *IEICE Tec. Rep.*, A-P2009-220, No. 3, pp. 91–94, 2010.
- 3 C. Ouchi, S. Fujii, and N. Wakai, "Solar-terrestrial disturbances of August 1972 15. Simultaneous measurement of intensities and phase of Loran-C waves," *Rev. RRL.*, Vol. 19, No. 103, pp. 367–372, 1973.
- 4 T. Ishimine and Y. Echizenya, "The short distance propagation of radio waves of frequency 40 kHz - Peculiar aspects of propagation of the low frequency radio waves on winter anomaly days," *Rev. RRL*, Vol. 29, No. 151, pp. 395–407, 1983.
- 5 Recommendation ITU-R P. 684-5, "Prediction of field strength at frequencies below 150 kHz," ITU, 2009.
- 6 N. Kurihara, A. Otsuka, K. Imamura, Y. Takahashi, and N. Wakai, "Nation-wide survey for measuring LF wave field strengths in winter," *IEICE Tec. Rep.*, A-P2004-195, pp. 29–34, 2004.
- 7 N. Wakai, N. Kurihara, A. Otsuka, K. Imamura, and Y. Takahashi, "Wintertime survey of LF field strengths in Japan," *Radio Sci.*, Vol. 41, No. 5, RS5S13, pp. 1–7, Sep./Oct. 2006.
- 8 J.S. Belrose, "Low and very low frequency radio wave propagation, in Radio wave Propagation," *AGARD Lecture Ser.*, Vol. 29, pp. 97–115, *Advis. Group for Aerosp. Res. And Dev.*, NATO, Neuilly-sur-Seine, France, 1968.
- 9 N. Wakai, N. Kurihara, A. Otsuka, and K. Imamura, "Prediction method of LF/MF field strengths," *IEICE Tec. Rep.*, A-P2003-271, pp. 35–40, 2004.
- 10 Recommendation ITU-R P. 684-4, "Prediction of field strength at frequencies below 150 kHz," ITU, 2005.
- 11 S. Tsuchiya, K. Nozaki, K. Imamura, H. Maeno, and N. Wakai, "Mobile measurements of the field strength of LF standard frequency waves on Asian and Transpacific routes," *IEICE Tec. Rep.*, A-P2007-138, pp. 93–98, 2008.
- 12 K. Nozaki, S. Tsuchiya, K. Imamura, H. Maeno, N. Nagahama, M. Umetsu, and N. Wakai, "Propagation experiments and Prediction Method of LF standard frequency waves," *IEICE Trans. Comm.*, Vol. J92-B, No. 12, pp. 1832–1843, 2009.
- 13 Y. Maekawa, K. Hamaguchi, M. Ishii, K. Nozaki, and A. Sato, "Radiowave propagation models for fixed systems and dynamics," *Jour. IEICE*, Vol. 93, No. 12, pp. 1015–1019, 2010.
- 14 Recommendation ITU-R P. 368-7, "Ground-wave propagation curves for frequencies between 10 kHz and 30 MHz," ITU, 1992.
- 15 Report ITU-R P. 1008, "Reflection from the surface of the Earth," ITU, 1986.
- 16 Recommendation ITU-R P. 1239, "ITU-R Reference ionospheric characteristics, Annex I Ionospheric characteristics, 4 Prediction of foE," ITU, 2002
- 17 Recommendation ITU-R P. 372-9, "Radio Noise," ITU, 2007.
- 18 M. Iwama, T. Shinozuka, and Y. Yamanaka, "The effect of radio noise on standard frequency and time signal emissions in LF band," *IEEE Trans. FM*, Vol. 126, No. 9, pp. 895–901, 2006.
- 19 Recommendation ITU-R P.832-2, "World Atlas of Ground Conductivities," ITU-R, 1999.

(Accepted Oct. 28, 2010)



**TSUCHIYA Shigeru**

*Senior Researcher, Space-Time Standards Group, New Generation Network Research Center*

*Time and Frequency Standard, Radio Wave Propagation*



**IMAMURA Kuniyasu**

*Research Manager, Space-Time Standards Group, New Generation Network Research Center*

*Time and Frequency Standard*

**ITO Hiroyuki, Ph.D.**

*Senior Researcher, Space-Time Standards Group, New Generation Network Research Center*

*Atomic Frequency Standard, Optical Frequency Standards*



**MAENO Hideo, Ph.D.**

*Senior Researcher, Space-Time Standards Group, New Generation Network Research Center*

*Satellite Time Transfer*



**KUBOTA Minoru, Ph.D.**

*Senior Researcher, Space Environment Group, Applied Electromagnetic Research Center*

*Aeronomy*



**NOZAKI Kenro**

*Senior Engineer, Matsudo Laboratory, Telecom Engineering Center*

*Radio Science*